Adaptive Synchronized Control for Coordination of Multirobot Assembly Tasks

Dong Sun, *Member, IEEE*, and James K. Mills, *Member, IEEE*

***Abstract*—Coordination of multirobot systems has received extensive studies in the past decade. The majority of previous approaches require a complex setup of the hybrid position/force-control architecture, and have not fully addressed the coordination problem when the robots are not kinematically constrained but perform a common task. In this paper, we propose to use a new coordination scheme that is more straightforward and easier to implement and is applicable to a wider area. The basic idea of the new coordination strategy is to use the concept of motion synchronization, since the problem of coordinating multiple manipulators is basically the problem of maintaining certain kinematic relationships amongst robots. The key to the success of the new method is to ensure that each manipulator tracks its desired trajectory while synchronizing its motion with other manipulators' motions, so that differential (or synchronization) position errors amongst manipulators converge to zero. The controller, designed by incorporating the cross-coupling technology into an adaptive-control architecture, successfully guarantees asymptotic convergence to zero of both position tracking and synchronization errors simultaneously. Experiments and simulations on multirobot assembly systems demonstrate the effectiveness of the approach.**

***Index Terms*—Adaptive control, coordination, cross-coupling, multirobot, synchronization.**

I. Introduction

IT IS AN IMPORTANT issue to coordinate multiple robots in carrying out assembly tasks in modern manufacturing and space applications. So far, there mainly have been three kinds of coordination schemes reported in the literature. The first scheme is the master/slave control [1], [22], where one robot arm is under position control, and the others are subject to compliant force control to maintain kinematic constraints. The second scheme utilizes a centralized control architecture [7], [15], [17], [20], [21], in which robots and the grasped payload are considered as a closed kinematic chain. This method is designed based on a unified robot and payload dynamic model. The third scheme is a decentralized control [2], [5], [12], [18], in which each robot is controlled separately by its own local controller. All of these coordination schemes considered the common situation that multiple manipulators are physically connected together for assembly tasks (i.e., grasping a payload) and employ hybrid position and force controls.

In this paper, we consider a multirobot task in which the following conditions may hold. a) The robots are kinematically constrained, i.e., all robots grasp a common rigid payload. b) The robots are not physically connected, but perform a common task, i.e., one robot manipulates a rigid payload while another spreads adhesive on the edges, with both robots in motion simultaneously. c) A task in which two robots simultaneously spread adhesive on a single path for assembly. Conventional centralized and decentralized coordination schemes have not addressed coordination tasks of b) and c). While the master/slave control scheme may be realized as a solution to such coordination, the performance of the master/slave control may be adversely affected due to a communication delay existing amongst robots. There exists increasing demand for developing a new coordination scheme that is applicable to all coordination tasks mentioned above. Another motivation for developing a new coordination scheme arises from significant demand for easy and efficient implementation. Few coordination schemes so far can be easily applied in practice, due to a complex setup of the hybrid position and force-control architecture when implemented on commercially available robots.

Synchronized control provides a unique advantage and opportunity for multirobot coordination by maintaining certain kinematic relationships without explicitly employing internal force control amongst robots. Using the synchronization approach, manipulators are controlled in a synchronous manner so that tracking errors and synchronization errors converge to zero, where synchronization errors are defined to be differential position errors amongst manipulators. Note that the synchronization error is used to evaluate the degree of coordination. It is not equivalent to the tracking error. Most coordination tasks concern not only whether position errors converge to zero, but also how these position errors converge to zero. The consideration of synchronization errors in the proposed control design is aimed to regulate robot trajectories in the transient stage. An effective synchronization method in use is the so-called cross-coupling control, the concept first introduced by Koren [8]. The majority of the previous work on cross-coupling control was proposed mainly for machine tools, such as Kulkarni and Srinivasan [10], Tomizuka *et al.* [16], Koren and Lo [9], and Kamano *et al.* [6], etc. Other approaches include fuzzy logic coupling control (Moore and Chen [13]) and neurocontroller for synchronization (Lee and Jeon [11]).

Manuscript received July 14, 2001; revised January 25, 2002. This paper was recommended for publication by Associate Editor F. Cheng and Editor S. Hutchinson upon evaluation of the reviewers' comments. This work was supported in part by the Research Grants Council of the Hong Kong Special Administrative Region, China, under Project CityU 1085/01E and by City University of Hong Kong under Project 7001365. This paper was presented in part at the 2002 IEEE International Conference on Robotics and Automation, Washington, D.C., May 2002.

D. Sun is with the Department of Manufacturing Engineering and Engineering Management, City University of Hong Kong, Kowloon, Hong Kong (e-mail: medsun@cityu.edu.hk).

J. K. Mills is with the Department of Mechanical and Industrial Engineering, University of Toronto, Toronto, ON M5S 3G8 Canada (e-mail: mills@mie.utoronto.ca).

Digital Object Identifier 10.1109/TRA.2002.802229

The use of the cross-coupling control in robotics was performed by Feng *et al.* [3], where the differential velocity error of two driving wheels in a mobile vehicle was minimized through motion synchronization. The synchronization scheme was also applied in a distributed computing system, i.e., "tight" and "loose" coupling [4].

Adaptive control is an effective strategy used to address the synchronization problem. Tomizuka *et al.* [16] designed and implemented adaptive feedforward controllers for speed synchronization of two motions axes, which was followed by Yang and Chang [19] in synchronization of twin-gyro precession. However, the feedforward control approach is not ideal when the system is subject to a variable control environment and system nonlinearities. Also, the proposed feedforward adaptive synchronization deals with velocity synchronization only and fails to address the position synchronization problem. In this study, we propose to use a new adaptive coupling-control algorithm to synchronize positions of multiple manipulators for coordination. The cross-coupling technology is incorporated into an adaptive-control architecture through feedback of position and synchronization errors in both the controller and the parameter adaptor. Note that consideration of all synchronization errors in each robot control may result in intensive online computation work, especially when the number of manipulators is large. Therefore, the synchronization strategy proposed in this study is to stabilize synchronization errors between each manipulator and the other two manipulators (but not all other manipulators) to zero. This is based on an assumption that motions of all manipulators are synchronized if every pair of manipulators are synchronized in motion. The significance of the proposed coordination scheme is threefold.

1) Implementation of incorporation of the differential position error into an adaptive architecture for multirobot control is relatively straightforward. There is no need to explicitly employ hybrid position and force control in the controller design.
2) Position errors and synchronization error(s) converge to zero asymptotically, which has yet to be reported in the literature.
3) The controller is of a decentralized architecture and is able to address model uncertainties and external force disturbances.

II. Synchronization Function

Consider a robot assembly work cell with n manipulators. Denote $x_i(t)$ as the joint or Cartesian coordinates of robot manipulator i, where $i = 1 \sim n$. The position tracking error of the ith manipulator in following a desired position trajectory, $x_i^d(t)$, is given by

$$e_i(t) = x_i^d(t) - x_i(t). \tag{1}$$

The problem of coordinating multiple robots is basically the problem of maintaining a kinematic relationship amongst robots. Suppose that coordinated manipulators are subject to the following synchronization function, which in fact defines the task:

$$\Re\left\{(x_{1\sim n}(t))\,|f\left(x_1(t), x_2(t), \ldots, x_n(t)\right) = 0\right\}. \tag{2}$$

The function (2) is valid for all desired coordinates $x_i^d(t)$, namely

$$\Re\left\{\left(x_{1\sim n}^d(t)\right)\,|f\left(x_1^d(t), x_2^d(t), \ldots, x_n^d(t)\right) = 0\right\}. \tag{3}$$

Using a Taylor series expansion, $f(x_1(t), x_2(t), \ldots, x_n(t))$ can be expanded at the desired coordinates $x_i^d(t)$, i.e.

$$\begin{aligned} & f\left(x_1(t), x_2(t), \ldots, x_n(t)\right) \\ &= f\left(x_1^d(t), x_2^d(t), \ldots, x_n^d(t)\right) \\ &\quad + \sum_{i=1}^{n}\left[\frac{\partial f(\cdot)}{\partial x_i}\bigg|_{x_i^d}\left(x_i(t) - x_i^d(t)\right) + \mathcal{O}\left(x_i(t)\right)\right] \\ &= \sum_{i=1}^{n}\left[-\frac{\partial f(\cdot)}{\partial x_i}\bigg|_{x_i^d} e_i(t) + \mathcal{O}\left(x_i\right)\right] \end{aligned} \tag{4}$$

where $\mathcal{O}(x_i(t))$ denotes higher order terms. Then, the function (2) is equivalent to

$$\sum_{i=1}^{n}\left[c_i(t)e_i(t) + \mathcal{O}\left(x_i\right)\right] = 0 \tag{5}$$

where $c_i(t) = -\partial f(\cdot)/\partial x_i|_{x_i^d}$, denotes a diagonal coupling parameter regarding the first-order error $e_i(t)$. Note that $c_i(t)$ is bounded. To achieve the goal of coordination, (5) must be satisfied. In the following, we give several examples to show how to derive (5).

Example 1: Consider two manipulators holding a rigid object in a trajectory tracking task. Since it is a requirement that the difference between positions/orientations of two end-effectors of robots must remain constant so as not to damage the payload or robots, the position coordinates of two manipulators, denoted by $x_1(t)$ and $x_2(t)$, are subject to a synchronization function

$$f\left(x_1, x_2\right) = x_1(t) - x_2(t) - A = 0$$

where A is a constant vector. According to (5), the above function is equivalent to causing position errors $e_1(t)$ and $e_2(t)$ to satisfy

$$e_1(t) - e_2(t) = 0.$$

Example 2: Consider that a differential mobile robot with two driving wheels tracks a curved path. Radii of the desired curves the two driving wheels follow are denoted by $R_1(t)$ and $R_2(t)$, respectively. The displacements of two driving wheels, denoted by $x_1(t)$ and $x_2(t)$, are subject to a synchronization function

$$f\left(x_1, x_2\right) = \frac{x_1(t)}{R_1(t)} - \frac{x_2(t)}{R_2(t)} = 0$$

or

$$f\left(x_1, x_2\right) = R_2(t)x_1(t) - R_1(t)x_2(t) = 0.$$

From (5), the above function is equivalent to causing the displacement errors $e_1(t)$ and $e_2(t)$ to satisfy

$$c_1(t)e_1(t) + c_2(t)e_2(t) = 0$$

where $c_1(t) = -R_2(t)$ and $c_2(t) = R_1(t)$.

Example 3: Consider that two manipulators with coordinates $x_1(t)$ and $x_2(t)$ are subject to a synchronization function

$$f(x_1, x_2) = x_1^T(t)x_1(t) + x_2^T(t)x_2(t) - A = 0$$

where A is a constant vector. From (5), the above function is equivalent to causing position errors $e_1(t)$ and $e_2(t)$ to satisfy

$$c_1(t)e_1(t) + c_2(t)e_2(t) + c_1^{\{2\}}(t)e_1^T(t)e_1(t) + c_2^{\{2\}}(t)e_2^T(t)e_2(t) = 0$$

where $c_1(t) = -2x_1^d(t)^T$, $c_2(t) = -2x_2^d(t)^T$, $c_1^{\{2\}}(t) = -2$, and $c_2^{\{2\}}(t) = -2$.

It can be seen from the above examples that synchronization functions may contain coordinate errors in the first order (i.e., $e_1(t)$ and $e_2(t)$) or of the higher order (i.e., $e_1^T(t)e_1(t)$ and $e_2^T(t)e_2(t)$). Since it is more common that synchronization functions arisen from coordination tasks are linear functions of robot coordinates, we introduce the following assumption:

Assumption 1: In this paper, we investigate such case that the synchronization function $f(x_1, x_2, \ldots, x_n) = 0$, to which the robot manipulators are subject, is a linear function of variables $x_i(t)$.

Assumption 1 ensures a linear synchronization relationship with respect to robot coordinates. Under *Assumption 1*, the function (2) or (5) becomes

$$\sum_{i=1}^{n} c_i(t)e_i(t) = 0. \tag{6}$$

Note that the inverse of the diagonal coupling parameter $c_i(t)$ exists, since all elements of the coordinate vector $x_i(t)$ are related to elements of the other coordinates in the synchronization function $f(\cdot)$.

III. Coordination of Two Manipulators

Since coordination of two manipulators is common in robotics, we will first investigate this specific case using synchronization strategy. The approach will be extended to multiple manipulators in the next section.

We introduce a differential or synchronization error, $\epsilon(t)$, defined by

$$\epsilon(t) = c_1(t)e_1(t) + c_2(t)e_2(t). \tag{7}$$

To achieve the goal of the coordination, the synchronization function (2) or (5) must be satisfied. Hence, it is a requirement that the synchronization error $\epsilon(t) \to 0$ during the motion, in addition to achieving $e_1(t) \to 0$ and $e_2(t) \to 0$.

The dynamics of the ith manipulator are described by

$$H_i(x_i)\ddot{x}_i(t) + C_i(x_i, \dot{x}_i)\dot{x}_i(t) + F_i(x_i, \dot{x}_i) = \tau_i \tag{8}$$

where $H_i(x_i)$ denotes the inertia of manipulator i. $C_i(x_i, \dot{x}_i)$ denotes the effect of Coriolis, centrifugal, and other coupling terms. $F_i(x_i, \dot{x}_i)$ denotes the external disturbance. τ_i is the input torque. Note that $(1/2)\dot{H}_i(x_i) - C_i(x_i, \dot{x}_i)$ is a skew-symmetric matrix.

Define θ_i as the vector containing unknown dynamic model parameters in (8). Since it is not possible to determine θ_i exactly in practice, we define $\hat{\theta}_i(t)$ as the estimate of θ_i. The estimated dynamic model is thus given by

$$\begin{aligned}\hat{H}_i(x_i)\ddot{x}_i(t) + \hat{C}_i(x_i, \dot{x}_i)\dot{x}_i(t) + \hat{F}_i(x_i, \dot{x}_i) \\ = Y_i(x_i, \dot{x}_i, \ddot{x}_i)\hat{\theta}_i(t) = \tau_i\end{aligned} \tag{9}$$

where $Y_i(x_i, \dot{x}_i, \ddot{x}_i)$ denotes a regression matrix and $\hat{H}_i(x_i)$, $\hat{C}_i(x_i, \dot{x}_i)$, and $\hat{F}_i(x_i, \dot{x}_i)$ are estimates of $H_i(x_i)$, $C_i(x_i, \dot{x}_i)$, and $F_i(x_i, \dot{x}_i)$, respectively.

We introduce a new concept named *coupled position error*, denoted by $e_i^*(t)$. The coupled position error $e_i^*(t)$ contains the position error and the synchronization error, i.e.,

$$e_i^*(t) = c_i(t)e_i(t) + \beta \int_0^t \epsilon(w)dw \tag{10}$$

where β is a diagonal positive coupling parameter. Define a command vector as

$$u_i(t) = c_i(t)\dot{x}_i^d(t) + \dot{c}_i(t)e_i(t) + \beta\epsilon(t) + \Lambda e_i^*(t) \tag{11}$$

where Λ is a positive control gain. Definition of $u_i(t)$ in (11) leads to the following vector regarding the coupled position and velocity errors:

$$r_i(t) = u_i(t) - c_i(t)\dot{x}_i(t) = \dot{e}_i^*(t) + \Lambda e_i^*(t). \tag{12}$$

Now, the control objective is defined to design control torques to restrict $r_i(t)$ to lie on a sliding surface, so that the coupled errors $e_i^*(t)$ and $\dot{e}_i^*(t)$ tend to zero.

Design the input torques as follows, in a decentralized architecture:

$$\begin{aligned}\tau_i =& \hat{H}_i(x_i)c_i^{-1}(t)(\dot{u}_i(t) - \dot{c}_i(t)\dot{x}_i(t)) \\ &+ \hat{C}_i(x_i, \dot{x}_i)c_i^{-1}(t)u_i(t) + \hat{F}_i(x_i, \dot{x}_i) \\ &+ k_r c_i^{-1}(t)r_i(t) + c_i^T(t)k_\epsilon\epsilon(t) \\ =& Y_i(x_i, \dot{x}_i, u_i, \dot{u}_i)\hat{\theta}_i(t) + k_r c_i^{-1}(t)r_i(t) + c_i^T(t)k_\epsilon\epsilon(t)\end{aligned} \tag{13}$$

where k_r and k_ϵ are diagonal positive-control gains. Note that the regression matrix $Y_i(x_i, \dot{x}_i, u_i, \dot{u}_i)$ is now a function of u_i and $\dot{u}_i$, rather than $\ddot{x}_i$. The estimated parameter $\hat{\theta}_i(t)$ is subject to the adaptation law

$$\dot{\hat{\theta}}_i(t) = \Gamma_i Y_i^T(x_i, \dot{x}_i, u_i, \dot{u}_i)c_i^{-1}(t)r_i(t) \tag{14}$$

where Γ_i is a diagonal positive-definite control gain. Define the model estimation error as

$$\tilde{\theta}_i(t) = \theta_i - \hat{\theta}_i(t). \tag{15}$$

Then, the adaptation law (14) can be rewritten in another form as

$$\dot{\tilde{\theta}}_i(t) = -\Gamma_i Y_i^T\left(x_i, \dot{x}_i, u_i, \dot{u}_i\right) c_i^{-1}(t) r_i(t). \tag{16}$$

Substituting the controller (13) into the dynamic (8) leads to the closed-loop dynamics

$$\begin{aligned} H_i\left(x_i\right) c_i^{-1}(t)\dot{r}_i(t) &+ C_i\left(x_i, \dot{x}_i\right) c_i^{-1}(t) r_i(t) \\ &+ k_r c_i^{-1}(t) r_i(t) + c_i^T(t) k_\epsilon \epsilon(t) \\ =&\Delta H_i\left(x_i\right) c_i^{-1}(t)\left(\dot{u}_i(t) - \dot{c}_i(t)\dot{x}_i(t)\right) \\ &+ \Delta C_i\left(x_i, \dot{x}_i\right) c_i^{-1}(t) u_i(t) + \Delta F_i\left(x_i, \dot{x}_i\right) \\ =&Y_i\left(x_i, \dot{x}_i, u_i, \dot{u}_i\right)\tilde{\theta}_i(t) \end{aligned} \tag{17}$$

where $\Delta H_i(x_i) = H_i(x_i) - \hat{H}_i(x_i)$, $\Delta C_i(x_i, \dot{x}_i) = C_i(x_i, \dot{x}_i) - \hat{C}_i(x_i, \dot{x}_i)$, and $\Delta F_i(x_i, \dot{x}_i) = F_i(x_i, \dot{x}_i) - \hat{F}_i(x_i, \dot{x}_i)$. It will be shown in the following that the proposed adaptive coupling controllers (13) and (14) guarantee asymptotic convergence to zero of both position-tracking errors $e_i(t)$ and the synchronization error $\epsilon(t)$.

Theorem 1: If the control gain k_r is large enough to satisfy

$$\lambda_{\min}\left(k_r\right) \geq \lambda_{\max}\left(H_i\left(x_i\right)\frac{d\left(c_i^{-1}(t)\right)}{dt} c_i(t)\right) \tag{18}$$

where $\lambda_{\min}(\cdot)$ and $\lambda_{\max}(\cdot)$ denote the minimum and the maximum eigenvalues of matrices $(\cdot)$, respectively, then the proposed adaptive coupling controllers (13) and (14) give rise to asymptotic convergence to zero of position and synchronization errors, i.e., $e_i(t) \to 0$ and $\epsilon(t) \to 0$ as time $t \to \infty$.

Proof: Define a positive definite function as

$$\begin{aligned} V(t) = \sum_{i=1}^{2} &\left[\frac{1}{2} r_i^T(t) c_i^{-T}(t) H_i\left(x_i\right) c_i^{-1}(t) r_i(t)\right. \\ &\left. + \frac{1}{2}\tilde{\theta}_i^T(t)\Gamma_i^{-1}\tilde{\theta}_i(t)\right] + \frac{1}{2}\epsilon^T(t) k_\epsilon \epsilon(t) \\ &+ \left(\int_0^t \epsilon^T(w)dw\right) k_\epsilon \Lambda\beta \int_0^t \epsilon(w)dw. \end{aligned} \tag{19}$$

Differentiating $V(t)$ with respect to time yields

$$\begin{aligned} \dot{V}(t) = \sum_{i=1}^{2} &\left[r_i^T(t) c_i^{-T}(t) H_i\left(x_i\right) c_i^{-1}(t)\dot{r}_i(t)\right. \\ &+ \frac{1}{2} r_i^T(t) c_i^{-T}(t)\dot{H}_i\left(x_i\right) c_i^{-1}(t) r_i(t) \\ &+ r_i^T(t) c_i^{-T}(t) H_i\left(x_i\right)\frac{d\left(c_i^{-1}(t)\right)}{dt} r_i(t) \\ &\left. + \tilde{\theta}_i^T(t)\Gamma_i^{-1}\dot{\tilde{\theta}}_i(t)\right] \\ &+ \epsilon^T(t) k_\epsilon \dot{\epsilon}(t) + 2\epsilon^T(t) k_\epsilon \Lambda\beta \int_0^t \epsilon(w)dw. \end{aligned} \tag{20}$$

Multiplying both sides of the closed-loop equation (17) by $r_i^T(t) c_i^{-T}(t)$, and then substituting the resulting equation into (20) yields

$$\begin{aligned} \dot{V}(t) = \sum_{i=1}^{2} &\left[-r_i^T(t) c_i^{-T}(t) k_r c_i^{-1}(t) r_i(t)\right. \\ &+ r_i^T(t) c_i^{-T}(t) H_i\left(x_i\right)\frac{d\left(c_i^{-1}(t)\right)}{dt} r_i(t) \\ &+ \tilde{\theta}_i^T(t)\Gamma_i^{-1}\dot{\tilde{\theta}}_i(t) \\ &\left. + r_i^T(t) c_i^{-T}(t) Y_i^T\left(x_i, \dot{x}_i, u_i, \dot{u}_i\right)\tilde{\theta}_i(t)\right] \\ &- \left(r_1(t) + r_2(t)\right)^T k_\epsilon \epsilon(t) + \epsilon^T(t) k_\epsilon \dot{\epsilon}(t) \\ &+ 2\epsilon^T(t) k_\epsilon \Lambda\beta \int_0^t \epsilon(w)dw. \end{aligned} \tag{21}$$

From (16), we have

$$\tilde{\theta}_i^T(t)\Gamma_i^{-1}\dot{\tilde{\theta}}_i(t) + r_i^T(t) c_i^{-T}(t) Y_i^T\left(x_i, \dot{x}_i, u_i, \dot{u}_i\right)\tilde{\theta}_i(t) = 0. \tag{22}$$

From (7), (10), and (12), we have

$$r_1(t) + r_2(t) = \dot{\epsilon}(t) + (2\beta + \Lambda)\epsilon(t) + 2\beta\Lambda \int_0^t \epsilon(w)dw. \tag{23}$$

Substituting (22) and (23) into (21) yields

$$\begin{aligned} \dot{V}(t) = &-\sum_{i=1}^{2}\left\{r_i^T(t) c_i^{-T}(t)\left[k_r - H_i\left(x_i\right)\frac{d\left(c_i^{-1}(t)\right)}{dt} c_i(t)\right]\right. \\ &\left.\cdot c_i^{-1}(t) r_i(t)\right\} - \epsilon^T(t)(2\beta + \Lambda) k_\epsilon \epsilon(t) \\ \leq &-\sum_{i=1}^{2}\left[\lambda_{\min}\left(k_r\right) - \lambda_{\max}\left(H_i\left(x_i\right)\frac{d\left(c_i^{-1}(t)\right)}{dt} c_i(t)\right)\right] \\ &\cdot \left\|c_i^{-1}(t) r_i(t)\right\|^2 - \epsilon^T(t)(2\beta + \Lambda) k_\epsilon \epsilon(t) \end{aligned} \tag{24}$$

where $\lambda_{\min}(\cdot)$ and $\lambda_{\max}(\cdot)$ denote the minimum and the maximum eigenvalues of matrices $(\cdot)$, respectively. If k_r is large enough to satisfy (18), then $\dot{V}(t) \leq 0$. Hence, $c_i^{-1}(t) r_i(t)$ and $\epsilon(t)$ are bounded in terms of L_2 norm. Following (19) and (24), we conclude that $\tilde{\theta}_i(t)$ is bounded. Since $c_i^{-1}(t)$ is bounded, $r_i(t)$ is bounded. As a result, $\dot{e}_i^*(t)$ and $e_i^*(t)$ are bounded from (12) and so are $\dot{e}_i(t)$ by differentiating (10). $\dot{\epsilon}(t)$ is further bounded from differentiating (7). From (17), $c_i^{-1}(t)\dot{r}_i(t)$ is bounded, and thus, $\dot{r}_i(t)$ is bounded. Therefore, $r_i(t)$ and $\epsilon(t)$ are uniformly continuous, since $\dot{r}_i(t)$ and $\dot{\epsilon}(t)$ are all bounded. From Barbalat's lemma, it follows that $r_i(t) \to 0$ and $\epsilon(t) \to 0$ as time $t \to \infty$. From (12), $e_i^*(t) \to 0$ and $\dot{e}_i^*(t) \to 0$ as $t \to \infty$. From (7), we have

$$\epsilon(t) = c_1(t) e_1(t) + c_2(t) e_2(t) \to 0. \tag{25}$$

From (10), we have

$$e_1^*(t) - e_2^*(t) = c_1(t) e_1(t) - c_2(t) e_2(t) \to 0. \tag{26}$$

Combining (25) and (26) yields $c_1(t) e_1(t) \to 0$ and $c_2(t) e_2(t) \to 0$. Since the inverse of $c_i(t)$ exists, we finally conclude that $e_1(t) \to 0$ and $e_2(t) \to 0$ as time $t \to \infty$. ■

Theorem 1 indicates that two manipulators can be successfully coordinated through synchronizing manipulators' motions to maintain certain kinematic relationships between them. The key to the success of the proposed method lies in the ability to control coordinates of two manipulators while regulating the relationship between them, made possible by defining the synchronization function as a linear function of $e_1(t)$ and $e_2(t)$ under *Assumption 1*. Although the independent adaptive control without synchronization ensures that position errors $e_i(t) \to 0$ and eventually $\epsilon(t) \to 0$, the proposed synchronous control improves the transient performance of synchronization significantly.

IV. Coordination of Multiple Manipulators

In this section, we extend the motion synchronization strategy from two-manipulator coordination to multimanipulator coordination.

A. Synchronization Strategy

The goal of maintaining kinematic relationships amongst n manipulators, as given by (6), can be divided into n subgoals specified by

$$\begin{aligned} c_1(t)e_1(t) + c_2(t)e_2(t) &= 0 \\ c_2(t)e_2(t) + c_3(t)e_3(t) &= 0 \\ &\vdots \\ c_n(t)e_n(t) + c_1(t)e_1(t) &= 0. \end{aligned} \tag{27}$$

If all subgoals listed in (27) can be achieved, (6) is achieved. Define synchronization errors of a subset of all possible pairs of two manipulators from the total of n manipulators in the following way:

$$\begin{aligned} \epsilon_1(t) &= c_1(t)e_1(t) + c_2(t)e_2(t) \\ \epsilon_2(t) &= c_2(t)e_2(t) + c_3(t)e_3(t) \\ &\vdots \\ \epsilon_n(t) &= c_n(t)e_n(t) + c_1(t)e_1(t). \end{aligned} \tag{28}$$

Accordingly, the control objective is defined to design control torques $\begin{bmatrix} \tau_1(t) \\ \tau_2(t) \\ \vdots \\ \tau_n(t) \end{bmatrix}$ to cause position tracking errors $\begin{bmatrix} e_1(t) \\ e_2(t) \\ \vdots \\ e_n(t) \end{bmatrix}$ and synchronization errors $\begin{bmatrix} \epsilon_1(t) \\ \epsilon_2(t) \\ \vdots \\ \epsilon_n(t) \end{bmatrix}$ to converge to zero. Since all synchronization errors are related, the control of each manipulator must consider motion responses of other manipulators. However, including motion responses of all manipulators in the controller formulation of each manipulator may lead to intensive online computation work, especially when the number n is large. To solve this problem, we propose the following synchronization strategy.

Strategy: *The control torque applied to each manipulator is designed to stabilize the position tracking of this manipulator, while synchronizing motions between this manipulator and the other two manipulators with an adjacent sequence number. Specifically, the control torque τ_i for the ith manipulator is to control $e_i(t) \to 0$ and at the same time, to synchronize motions of the $(i-1)$th manipulator, the ith manipulator, and the $(i+1)$th manipulator, so that synchronization errors $\epsilon_{i-1}(t) \to 0$ and $\epsilon_i(t) \to 0$.*

Under the above strategy, motions of all manipulators are coordinated through synchronization. The control of each manipulator only additionally considers motion responses of the other two manipulators, but not all other manipulators, for synchronization. This significantly simplifies the implementation, especially when the number of manipulators is large.

B. Synchronized Control of Multiple Manipulators

Define coupled position errors $e_i^*(t)$ $(i = 1 \sim n)$ in the following way:

$$\begin{aligned} e_1^*(t) &= c_1(t)e_1(t) + \beta \int_0^t (\epsilon_1(w) + \epsilon_n(w))\, dw \\ e_2^*(t) &= c_2(t)e_2(t) + \beta \int_0^t (\epsilon_2(w) + \epsilon_1(w))\, dw \\ &\vdots \\ e_n^*(t) &= c_n(t)e_n(t) + \beta \int_0^t (\epsilon_n(w) + \epsilon_{n-1}(w))\, dw. \end{aligned} \tag{29}$$

Unlike the coupled position errors in (10) for two-manipulator systems, here each error $e_i^*(t)$ in (29) contains two synchronization errors. Define command vectors $u_i(t)$ as

$$\begin{aligned} u_1(t) &= c_1(t)\dot{x}_1^d(t) + \dot{c}_1(t)e_1(t) + \beta(\epsilon_1(t) + \epsilon_n(t)) + \Lambda e_1^*(t) \\ u_2(t) &= c_2(t)\dot{x}_2^d(t) + \dot{c}_2(t)e_2(t) + \beta(\epsilon_2(t) + \epsilon_1(t)) + \Lambda e_2^*(t) \\ &\vdots \\ u_n(t) &= c_n(t)\dot{x}_n^d(t) + \dot{c}_n(t)e_n(t) + \beta(\epsilon_n(t) + \epsilon_{n-1}(t)) \\ &\quad + \Lambda e_n^*(t). \end{aligned} \tag{30}$$

Then, we have these vectors regarding coupled position/velocity errors

$$\begin{aligned} r_1(t) &= u_1(t) - c_1(t)\dot{x}_1(t) = \dot{e}_1^*(t) + \Lambda e_1^*(t) \\ r_2(t) &= u_2(t) - c_2(t)\dot{x}_2(t) = \dot{e}_2^*(t) + \Lambda e_2^*(t) \\ &\vdots \\ r_n(t) &= u_n(t) - c_n(t)\dot{x}_n(t) = \dot{e}_n^*(t) + \Lambda e_n^*(t). \end{aligned} \tag{31}$$

Design input torques, in a decentralized architecture, as shown in (32) at the bottom of the next page, where the estimated parameters $\hat{\theta}_i(t)$ are subject to the adaptation law in the same form as in (14). Substituting (32) into the robot dynamics leads to the closed-loop equations

$$\begin{aligned} &H_1(x_1)c_1^{-1}(t)\dot{r}_1(t) + C_1(x_1, \dot{x}_1)\, c_1^{-1}(t)r_1(t) \\ &\qquad + k_r c_1^{-1}(t)r_1(t) + c_1^T(t)k_\epsilon(\epsilon_1(t) + \epsilon_n(t)) \\ &\quad = Y_1(x_1, \dot{x}_1, u_1, \dot{u}_1)\,\tilde{\theta}_1(t) \\ &H_2(x_2)c_2^{-1}(t)\dot{r}_2(t) + C_2(x_2, \dot{x}_2)\, c_2^{-1}(t)r_2(t) \\ &\qquad + k_r c_2^{-1}(t)r_2(t) + c_2^T(t)k_\epsilon(\epsilon_2(t) + \epsilon_1(t)) \end{aligned}$$

$$
\begin{aligned}
&=Y_2\left(x_2,\dot{x}_2,u_2,\dot{u}_2\right)\tilde{\theta}_2(t)\\
&\vdots\\
&H_n\left(x_n\right)c_n^{-1}(t)\dot{r}_n(t)+C_n\left(x_n,\dot{x}_n\right)c_n^{-1}(t)r_n(t)\\
&\quad+k_rc_n^{-1}(t)r_n(t)+c_n^T(t)k_\epsilon\left(\epsilon_n(t)+\epsilon_{n-1}(t)\right)\\
&=Y_n\left(x_n,\dot{x}_n,u_n,\dot{u}_n\right)\tilde{\theta}_n(t). \qquad (33)
\end{aligned}
$$

Theorem 2: If the control gain k_r is large enough to satisfy (18) for each manipulator, the proposed adaptive synchronized controllers guarantee asymptotic convergence to zero of position errors and synchronization errors, i.e., $e_i(t)\rightarrow 0$ and $\epsilon_i(t)\rightarrow 0$ as time $t\rightarrow\infty$.

Proof: Define a positive-definite function as

$$
\begin{aligned}
V(t)=&\sum_{i=1}^{n}\left[\frac{1}{2}r_i^T(t)c_i^{-T}(t)H_i\left(x_i\right)c_i^{-1}(t)r_i(t)\right.\\
&\left.+\frac{1}{2}\tilde{\theta}_i^T(t)\Gamma_i^{-1}\tilde{\theta}_i(t)+\frac{1}{2}\epsilon_i^T(t)k_\epsilon\epsilon_i(t)\right]\\
&+\frac{1}{2}\left(\int_0^t\left(\epsilon_1(w)+\epsilon_n(w)\right)^T dw\right)k_\epsilon\Lambda\beta\\
&\cdot\int_0^t\left(\epsilon_1(w)+\epsilon_n(w)\right)dw\\
&+\sum_{i=2}^{n}\frac{1}{2}\left(\int_0^t\left(\epsilon_i(w)+\epsilon_{i-1}(w)\right)^T dw\right)k_\epsilon\Lambda\beta\\
&\cdot\int_0^t\left(\epsilon_i(w)+\epsilon_{i-1}(w)\right)dw. \qquad (34)
\end{aligned}
$$

Differentiating $V(t)$ with respect to time yields

$$
\begin{aligned}
\dot{V}(t)=&\sum_{i=1}^{n}\left[r_i^T(t)c_i^{-T}(t)H_i\left(x_i\right)c_i^{-1}(t)\dot{r}_i(t)\right.\\
&+\frac{1}{2}r_i^T(t)c_i^{-T}(t)\dot{H}_i\left(x_i\right)c_i^{-1}(t)r_i(t)\\
&+r_i^T(t)c_i^{-T}(t)H_i\left(x_i\right)\frac{d\left(c_i^{-1}(t)\right)}{dt}r_i(t)\\
&\left.+\tilde{\theta}_i^T(t)\Gamma_i^{-1}\dot{\tilde{\theta}}_i(t)+\epsilon_i^T(t)k_\epsilon\dot{\epsilon}_i(t)\right]\\
&+\left(\epsilon_1(t)+\epsilon_n(t)\right)^T k_\epsilon\Lambda\beta\int_0^t\left(\epsilon_1(w)+\epsilon_n(w)\right)dw\\
&+\sum_{i=2}^{n}\left(\epsilon_i(t)+\epsilon_{i-1}(t)\right)^T k_\epsilon\Lambda\beta\int_0^t\left(\epsilon_i(w)+\epsilon_{i-1}(w)\right)dw. \qquad (35)
\end{aligned}
$$

Multiplying both sides of the closed-loop equations (33) by $r_i^T(t)c_i^{-T}(t)$, and then substituting the resulting equations into (35), we have

$$
\begin{aligned}
\dot{V}(t)=&\sum_{i=1}^{n}\left[r_i^T(t)c_i^{-T}(t)H_i\left(x_i\right)\frac{d\left(c_i^{-1}(t)\right)}{dt}r_i(t)\right.\\
&-r_i^T(t)c_i^{-T}(t)k_rc_i^{-1}(t)r_i(t)+\tilde{\theta}_i^T(t)\Gamma_i^{-1}\dot{\tilde{\theta}}_i(t)\\
&+r_i^T(t)c_i^{-T}(t)Y_i\left(x_i,\dot{x}_i,u_i,\dot{u}_i\right)\tilde{\theta}_i(t)\\
&\left.+\epsilon_i^T(t)k_\epsilon\dot{\epsilon}_i(t)\right]\\
&-\sum_{i=1}^{n-1}\left(r_i(t)+r_{i+1}(t)\right)^T k_\epsilon\epsilon_i(t)\\
&-\left(r_n(t)+r_1(t)\right)^T k_\epsilon\epsilon_n(t)\\
&+\left(\epsilon_1(t)+\epsilon_n(t)\right)^T k_\epsilon\Lambda\beta\int_0^t\left(\epsilon_1(w)+\epsilon_n(w)\right)dw\\
&+\sum_{i=2}^{n}\left(\epsilon_i(t)+\epsilon_{i-1}(t)\right)^T k_\epsilon\Lambda\beta\int_0^t\left(\epsilon_i(w)+\epsilon_{i-1}(w)\right)dw. \qquad (36)
\end{aligned}
$$

In view of (28), (29), and (31), we have

$$
\begin{aligned}
r_1(t)+r_2(t)=&\dot{\epsilon}_1(t)+\Lambda\epsilon_1(t)+\beta\left(2\epsilon_1(t)+\epsilon_2(t)+\epsilon_n(t)\right)\\
&+\Lambda\beta\int_0^t\left(2\epsilon_1(w)+\epsilon_2(w)+\epsilon_n(w)\right)dw\\
r_2(t)+r_3(t)=&\dot{\epsilon}_2(t)+\Lambda\epsilon_2(t)+\beta\left(2\epsilon_2(t)+\epsilon_3(t)+\epsilon_1(t)\right)\\
&+\Lambda\beta\int_0^t\left(2\epsilon_2(w)+\epsilon_3(w)+\epsilon_1(w)\right)dw\\
&\vdots\\
r_n(t)+r_1(t)=&\dot{\epsilon}_n(t)+\Lambda\epsilon_n(t)+\beta\left(2\epsilon_n(t)+\epsilon_1(t)+\epsilon_{n-1}(t)\right)\\
&+\Lambda\beta\int_0^t\left(2\epsilon_n(w)+\epsilon_1(w)+\epsilon_{n-1}(w)\right)dw. \qquad (37)
\end{aligned}
$$

$$
\begin{aligned}
\tau_1=&\hat{H}_1\left(x_1\right)c_1^{-1}(t)\left(\dot{u}_1(t)-\dot{c}_1(t)\dot{x}_1(t)\right)+\hat{C}_1\left(x_1,\dot{x}_1\right)c_1^{-1}(t)u_1(t)\\
&+\hat{F}_1\left(x_1,\dot{x}_1\right)+k_rc_1^{-1}(t)r_1(t)+c_1^T(t)k_\epsilon\left(\epsilon_1(t)+\epsilon_n(t)\right)\\
=&Y_1\left(x_1,\dot{x}_1,u_1,\dot{u}_1\right)\hat{\theta}_1(t)+k_rc_1^{-1}(t)r_1(t)+c_1^T(t)k_\epsilon\left(\epsilon_1(t)+\epsilon_n(t)\right)\\
\tau_2=&\hat{H}_2\left(x_2\right)c_2^{-1}(t)\left(\dot{u}_2(t)-\dot{c}_2(t)\dot{x}_2(t)\right)+\hat{C}_2\left(x_2,\dot{x}_2\right)c_2^{-1}(t)u_2(t)\\
&+\hat{F}_2\left(x_2,\dot{x}_2\right)+k_rc_2^{-1}(t)r_2(t)+c_2^T(t)k_\epsilon\left(\epsilon_2(t)+\epsilon_1(t)\right)\\
=&Y_2(x_2,\dot{x}_2,u_2,\dot{u}_2)\hat{\theta}_2(t)+k_rc_2^{-1}(t)r_2(t)+c_2^T(t)k_\epsilon\left(\epsilon_2(t)+\epsilon_1(t)\right)\\
&\vdots\\
\tau_n=&\hat{H}_n\left(x_n\right)c_n^{-1}(t)\left(\dot{u}_n(t)-\dot{c}_n(t)\dot{x}_n(t)\right)+\hat{C}_n\left(x_n,\dot{x}_n\right)c_n^{-1}(t)u_n(t)\\
&+\hat{F}_n\left(x_n,\dot{x}_n\right)+k_rc_n^{-1}(t)r_n(t)+c_n^T(t)k_\epsilon\left(\epsilon_n(t)+\epsilon_{n-1}(t)\right)\\
=&Y_n\left(x_n,\dot{x}_n,u_n,\dot{u}_n\right)\hat{\theta}_n(t)+k_rc_n^{-1}(t)r_n(t)+c_n^T(t)k_\epsilon\left(\epsilon_n(t)+\epsilon_{n-1}(t)\right) \qquad (32)
\end{aligned}
$$

As a result

$$\begin{aligned}
&\sum_{i=1}^{n-1}\left(r_i(t)+r_{i+1}(t)\right)^T k_\epsilon\epsilon_i(t)+\left(r_n(t)+r_1(t)\right)^T k_\epsilon\epsilon_n(t)\\
&=\sum_{i=1}^{n}\left[\epsilon_i^T(t)k_\epsilon\dot{\epsilon}_i(t)+\epsilon_i^T(t)k_\epsilon\Lambda\epsilon_i(t)\right]\\
&\quad+\left[2\sum_{i=1}^{n}\epsilon_i^T(t)k_\epsilon\beta\epsilon_i(t)+2\epsilon_1^T(t)k_\epsilon\beta\epsilon_2(t)\right.\\
&\qquad\left.+2\epsilon_2^T(t)k_\epsilon\beta\epsilon_3(t)+\cdots+2\epsilon_n^T(t)k_\epsilon\beta\epsilon_1(t)\right]\\
&\quad+2\sum_{i=1}^{n}\epsilon_i^T(t)k_\epsilon\Lambda\beta\int_0^t\epsilon_i(w)dw+\epsilon_1^T(t)k_\epsilon\Lambda\beta\int_0^t\epsilon_2(w)dw\\
&\quad+\epsilon_2^T(t)k_\epsilon\Lambda\beta\int_0^t\epsilon_1(w)dw+\epsilon_2^T(t)k_\epsilon\Lambda\beta\int_0^t\epsilon_3(w)dw\\
&\quad+\epsilon_3^T(t)k_\epsilon\Lambda\beta\int_0^t\epsilon_2(w)dw+\cdots\\
&\quad+\epsilon_n^T(t)k_\epsilon\Lambda\beta\int_0^t\epsilon_1(w)dw+\epsilon_1^T(t)k_\epsilon\Lambda\beta\int_0^t\epsilon_n(w)dw\\
&=\sum_{i=1}^{n}\left[\epsilon_i^T(t)k_\epsilon\dot{\epsilon}_i(t)+\epsilon_i^T(t)k_\epsilon\Lambda\epsilon_i(t)\right]\\
&\quad+\left(\epsilon_1(t)+\epsilon_n(t)\right)^T k_\epsilon\beta\left(\epsilon_1(t)+\epsilon_n(t)\right)\\
&\quad+\sum_{i=2}^{n}\left(\epsilon_i(t)+\epsilon_{i-1}(t)\right)^T k_\epsilon\beta\left(\epsilon_i(t)+\epsilon_{i-1}(t)\right)\\
&\quad+\left(\epsilon_1(t)+\epsilon_n(t)\right)^T k_\epsilon\Lambda\beta\int_0^t\left(\epsilon_1(w)+\epsilon_n(w)\right)dw\\
&\quad+\sum_{i=2}^{n}\left(\epsilon_i(t)+\epsilon_{i-1}(t)\right)^T k_\epsilon\Lambda\beta\int_0^t\left(\epsilon_i(w)+\epsilon_{i-1}(w)\right)dw.
\end{aligned}\tag{38}$$

Substituting (22) and (38) into (36) yields

$$\begin{aligned}
\dot{V}(t)=&-\sum_{i=1}^{n}r_i^T(t)c_i^{-T}(t)\left[k_r-H_i\left(x_i\right)\frac{d\left(c_i^{-1}(t)\right)}{dt}c_i(t)\right]\\
&\cdot c_i^{-1}(t)r_i(t)\\
&-\sum_{i=1}^{n}\epsilon_i^T(t)k_\epsilon\Lambda\epsilon_i(t)\\
&-\left(\epsilon_1(t)+\epsilon_n(t)\right)^T k_\epsilon\beta\left(\epsilon_1(t)+\epsilon_n(t)\right)\\
&-\sum_{i=2}^{n}\left(\epsilon_i(t)+\epsilon_{i-1}(t)\right)^T k_\epsilon\beta\left(\epsilon_i(t)+\epsilon_{i-1}(t)\right)\\
\le&-\sum_{i=1}^{n}\left[\lambda_{\min}\left(k_r\right)-\lambda_{\max}\left(H_i\left(x_i\right)\frac{d\left(c_i^{-1}(t)\right)}{dt}c_i(t)\right)\right]\\
&\cdot\left\|c_i^{-1}(t)r_i(t)\right\|^2\\
&-\sum_{i=1}^{n}\epsilon_i^T(t)k_\epsilon\Lambda\epsilon_i(t)-\left(\epsilon_1(t)+\epsilon_n(t)\right)^T\\
&\cdot k_\epsilon\beta\left(\epsilon_1(t)+\epsilon_n(t)\right)\\
&-\sum_{i=2}^{n}\left(\epsilon_i(t)+\epsilon_{i-1}(t)\right)^T k_\epsilon\beta\left(\epsilon_i(t)+\epsilon_{i-1}(t)\right).
\end{aligned}\tag{39}$$

If k_r is large enough to satisfy (18), $\dot{V}(t)\le 0$. Since $c_i^{-1}(t)r_i(t)$ and $\epsilon_i(t)$ appear in (39), they are both bounded in terms of L_2 norm. Following (34) and (39), we know that $\tilde{\theta}_i(t)$ is bounded. Since $c_i^{-1}(t)$ is bounded, $r_i(t)$ is bounded. As a result, $\dot{e}_i^*(t)$ and $e_i^*(t)$ are bounded from (31), and so are $\dot{e}_i$ by differentiating (29). Thus, $\dot{\epsilon}_i(t)$ are bounded from differentiating (28). From (33), $c_i^{-1}(t)\dot{r}_i(t)$ are bounded, and so are $\dot{r}_i(t)$. Therefore, $r_i(t)$ and $\epsilon_i(t)$ are uniformly continuous since $\dot{r}_i(t)$ and $\dot{\epsilon}_i(t)$ are bounded. From Barbalat's lemma, $r_i(t)\to 0$ and $\epsilon_i(t)\to 0$ as time $t\to\infty$. It then follows from (31) that $e_i^*(t)\to 0$ and $\dot{e}_i^*(t)\to 0$ as $t\to\infty$.

Now, we prove $e_i(t)\to 0$. When $\epsilon_i(t)=0$ for all $i=1\sim n$, we have

$$\epsilon_1(t)+\epsilon_2(t)+\cdots+\epsilon_n(t)=0.\tag{40}$$

Combing all equations in (28) and utilizing (40) yields

$$c_1(t)e_1(t)+c_2(t)e_2(t)+\cdots+c_n(t)e_n(t)=0.\tag{41}$$

Combing all equations in (29) and utilizing (41), we further obtain

$$\int_0^t\left(\epsilon_1(w)+\epsilon_2(w)+\cdots+\epsilon_n(w)\right)dw=0.\tag{42}$$

On the other hand, we combine equations in (29) in different way, i.e.

$$\begin{aligned}
&c_1(t)e_1(t)-c_2(t)e_2(t)-c_3(t)e_3(t)-\cdots-c_n(t)e_n(t)\\
&\quad=-2\beta\int_0^t\left(\epsilon_2(w)+\epsilon_3(w)+\cdots+\epsilon_{n-1}(w)\right)dw\\
&\quad=-2\beta\int_0^t\left(\epsilon_1(w)+\epsilon_2(w)+\epsilon_3(w)+\cdots+\epsilon_n(w)\right)dw\\
&\quad=0.
\end{aligned}\tag{43}$$

In a similar manner to (43), we can obtain

$$\begin{aligned}
&-c_1(t)e_1(t)+c_2(t)e_2(t)-c_3(t)e_3(t)\\
&\qquad-\cdots-c_n(t)e_n(t)=0\\
&-c_1(t)e_1(t)-c_2(t)e_2(t)+c_3(t)e_3(t)\\
&\qquad-\cdots-c_n(t)e_n(t)=0\\
&\qquad\vdots\\
&-c_1(t)e_1(t)-c_2(t)e_2(t)-c_3(t)e_3(t)\\
&\qquad-\cdots+c_n(t)e_n(t)=0.
\end{aligned}\tag{44}$$

Solving (41), (43), and (44), we have $c_i(t)e_i(t)=0$. Since $c_i^{-1}(t)$ exists, $e_i(t)=0$. Therefore, the invariant set of the closed-loop dynamics (33) in the set $\Omega=\{(x_i,\dot{x}_i):\dot{V}(t)=0\}$ contains zero position errors (i.e., $e_i(t)=0$). Using LaSalle's theorem, we finally conclude that $e_i(t)\to 0$ as time $t\to\infty$. ■

V. Case Studies

A. Experiments on Coordinating Two Industrial Robots

To demonstrate the validity of the proposed synchronization scheme for robot coordination, an experimental evaluation was performed on two commercially available A460 six-degrees-of-freedom (DOF) light industrial robots manufactured by CRS

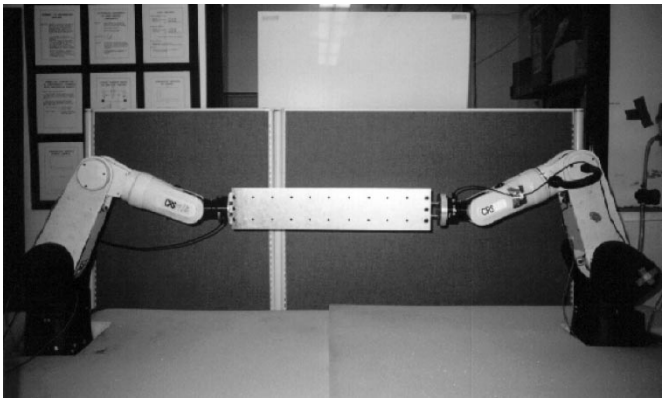

Fig. 1. Experimental setup of two CRS A460 robots.

TABLE I
JOINT ANGLES OF ROBOTS (UNIT: DEGREE)

	$\phi_1(1)$	$\phi_1(2)$	$\phi_1(3)$	$\phi_2(1)$	$\phi_2(2)$	$\phi_2(3)$
initial	73.3340	60.3330	-169.8120	15.2520	71.6830	-181.9800
final	90	63.6090	-174.7290	-2.9730	74.1070	-185.1080

Robotics Corporation. A setup of two robots manipulating a payload is shown in Fig. 1. Due to the limitation of the available computing hardware in the laboratory, the control scheme was implemented on the first three joints of each robot, and the remaining last three joints were position controlled with a proportional, integral, and derivative (PID) controller. For simplicity, we treated the last three links of each robot as a lumped mass attached at the end of link three of each robot, which allowed us to consider the dynamic model of the robot with the first three joints only. The actual joint angles were measured by encoders installed on each joint. The robots were controlled with a transputer-based C500 controller, supplied by CRS. A custom-designed experimental interface permits experiment setup, data collection, and display.

The dynamic model of the CRS A460 robot in the laboratory and the model formulation in terms of uncertain model parameters have been given in detail in our previous work [14]. The task implemented in the experiment was to move two robots along desired trajectories while causing the differential position error to be zero. Since the control law was executed in joint space in the experimental setup, we synchronized joint angles of robots and defined the following synchronization error

$$\epsilon(t) = e_1(t) - e_2(t) \quad \left(\epsilon(t) \in \Re^{3\times 1}\right). \tag{45}$$

Table I illustrates joint angles of the two manipulators in the initial and the final desired positions, respectively. The desired trajectory of each robot from the initial position to the final position is designed as a cubic polynomial. The control gains for each manipulator are: $\Lambda = \text{diag}\{8\}$ (1/s), $\beta = \text{diag}\{8\}$ (1/s), $k_r = \text{diag}\{80, 80, 100\}$ (N · m · s/rad), $k_\epsilon = \text{diag}\{10\}$ (N · m/rad · s), and $\Gamma = \text{diag}\{0.3\}$.

Figs. 2 and 3 illustrate actual joint angles (solid lines) following desired joint trajectories (dashdot lines) of the two manipulators, respectively. Fig. 4 illustrates synchronization (or differential) errors of the two robots at three joints. Due to the effects caused by friction and gravity, there exist residual offsets in the robot positions. To show the effectiveness of the proposed

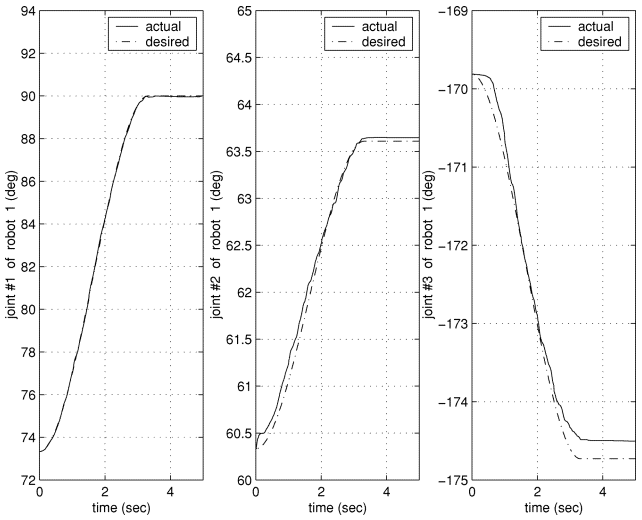

Fig. 2. Joint trajectories of robot 1 with adaptive synchronized control.

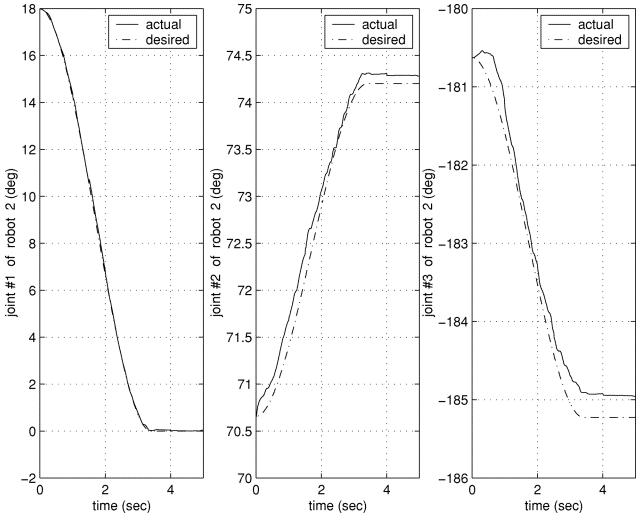

Fig. 3. Joint trajectories of robot 2 with adaptive synchronized control.

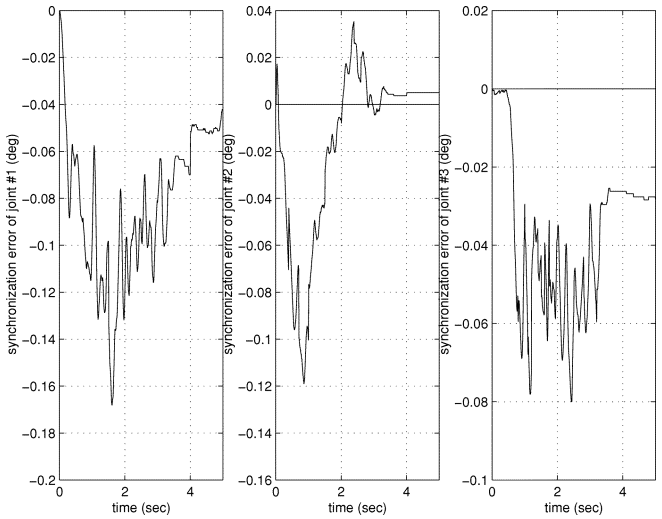

Fig. 4. Synchronization errors of robot joints with adaptive synchronized control.

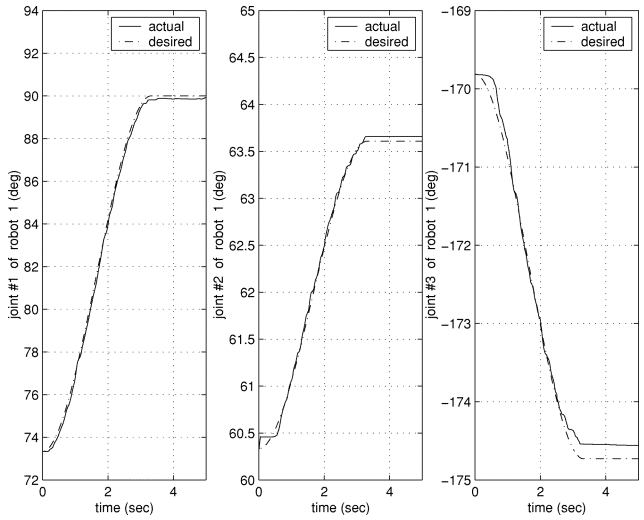

Fig. 5. Joint trajectories of robot 1 with independent adaptive control without synchronization.

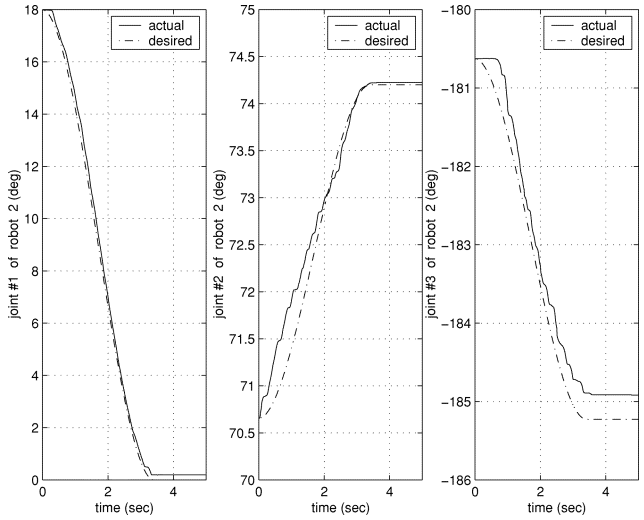

Fig. 6. Joint trajectories of robot 2 with independent adaptive control without synchronization.

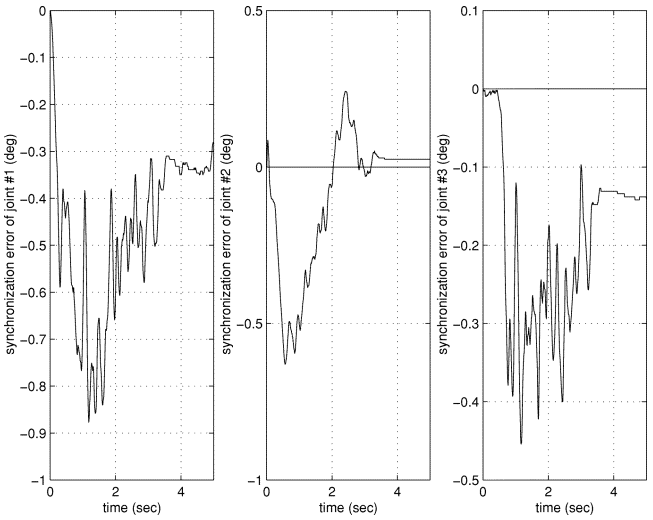

Fig. 7. Synchronization errors of robot joints with independent adaptive control without synchronization.

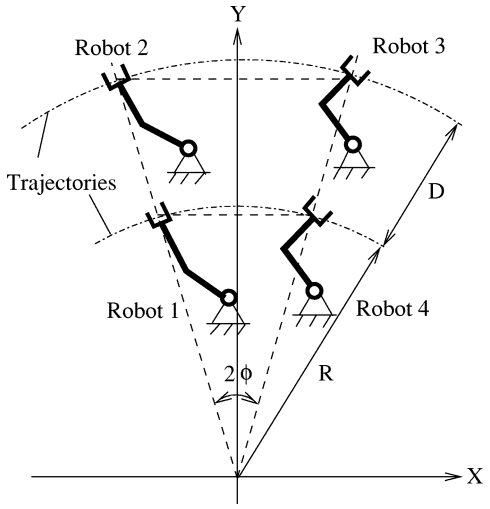

Fig. 8. Four planner manipulators in an assembly task.

synchronization control method, we further tested the system with the independent adaptive control without synchronization (namely $\beta = 0$ and $k_\epsilon = 0$) for comparison. Figs. 5 and 6 illustrate the actual and the desired joint angles of the two robots, respectively. Fig. 7 illustrates synchronization errors between two robots. It can be seen that although the independent control without synchronization could achieve satisfactory performance in each robot tracking, it exhibits poor coordination due to the large synchronization error. In contrast, the proposed synchronized controller exhibits much smaller synchronization errors (see Fig. 4), and therefore, exhibits better coordination ability.

B. Simulations on Coordinating Four Manipulators

We further applied the proposed coordination algorithm in simulating a robot work cell that contains four planar two-link manipulators, as shown in Fig. 8. The manipulators of the work cell were required to move along desired circular trajectories while maintaining a constant distance between each other. Specifically, every two adjacent robots must be required to meet the following kinematic relationship:

$$\begin{aligned}(R+D)e_1(t) - Re_2(t) &= 0\\ -Re_2(t) + Re_3(t) &= 0\\ Re_3(t) - (R+D)e_4(t) &= 0\\ -(R+D)e_4(t) + (R+D)e_1(t) &= 0\end{aligned} \tag{46}$$

where R and $R+D$ represent radii of the desired trajectories for robots 1, 4, and robots 2, 3, respectively. In the simulation, we selected $R = 5$ m and $D = 1$ m. Rewrite the relationship in (46) as

$$c_1e_1(t) + c_2e_2(t) + c_3e_3(t) + c_4e_4(t) = 0 \tag{47}$$

where $c_1 = R+D$, $c_2 = -R$, $c_3 = R$, and $c_4 = -(R+D)$. Consequently, the synchronization errors are defined as

$$\begin{aligned}\epsilon_1(t) &= c_1e_1(t) + c_2e_2(t)\\ \epsilon_2(t) &= c_2e_2(t) + c_3e_3(t)\\ \epsilon_3(t) &= c_3e_3(t) + c_4e_4(t)\\ \epsilon_4(t) &= c_4e_4(t) + c_1e_1(t).\end{aligned} \tag{48}$$

TABLE II
ROBOTS INITIAL AND FINAL POSITIONS

	initial positions $x_i(0)$ (unit: m)	final positions $x_i(f)$ (unit: m)
Robot 1	$[-R\sin\phi, R\cos\phi]^T$	$[-R\sin(\phi-0.02), R\cos(\phi-0.02)]^T$
Robot 2	$[-(R+D)\sin\phi, (R+D)\cos\phi]^T$	$[-(R+D)\sin(\phi-0.02), (R+D)\cos(\phi-0.02)]^T$
Robot 3	$[R\sin\phi, R\cos\phi]^T$	$[R\sin(\phi+0.02), R\cos(\phi+0.02)]^T$
Robot 4	$[(R+D)\sin\phi, (R+D)\cos\phi]^T$	$[(R+D)\sin(\phi+0.02), (R+D)\cos(\phi+0.02)]^T$

TABLE III
ROBOT CONFIGURATION AND MODEL PARAMETERS

	initial configuration	link length	link mass
Robot 1	$[\frac{2}{3}\pi, -\frac{1}{6}\pi)]^T$	$l_1 = l_2 = 0.3\text{m}$	$m_1 = m_2 = 1$ kg
Robot 2	$[\frac{2}{3}\pi, -\frac{1}{6}\pi)]^T$	$l_1 = l_2 = 0.3\text{m}$	$m_1 = m_2 = 1$ kg
Robot 3	$[\frac{2}{3}\pi, -\frac{1}{3}\pi)]^T$	$l_1 = l_2 = 0.3\text{m}$	$m_1 = m_2 = 1$ kg
Robot 4	$[\frac{2}{3}\pi, -\frac{1}{3}\pi)]^T$	$l_1 = l_2 = 0.3\text{m}$	$m_1 = m_2 = 1$ kg

The desired trajectory of each robot end-effector is given in the Cartesian space, specified by

$$x_i^d = x_i(0) + (x_i(f) - x_i(0))\,(1 - \exp(-t))\;\; (i = 1 \sim 4) \tag{49}$$

where $x_i(0)$ and $x_i(f)$, as given in Table II, denote the initial and the final desired positions, respectively. Table III illustrates initial configurations, link lengths, and link masses of the four robots. In the simulation, we assumed that the length and the mass of each link of robots are not known exactly. The uncertain parameter vector θ for each robot was defined by

$$\theta = \begin{bmatrix} \frac{1}{3}m_1 l_1^2 + m_2 l_1^2 \\ \frac{1}{3}m_2 l_2^2 \\ \frac{1}{2}m_2 l_1 l_2 \end{bmatrix}. \tag{50}$$

The regression matrix $Y = \begin{bmatrix} Y_{11} & Y_{12} & Y_{13} \\ Y_{21} & Y_{22} & Y_{23} \end{bmatrix}$ is specified by

$$\begin{aligned} Y_{11} =& z_1(1) \\ Y_{12} =& z_1(1) + z_1(2) \\ Y_{13} =& 2z_1(1)\cos q_2 + z_1(2)\cos q_2 - \dot{q}_2 z_2(1)\sin q_2 \\ & - (\dot{q}_1 + \dot{q}_2)\, z_2(2)\sin q_2 \\ Y_{21} =& 0 \\ Y_{22} =& z_1(1) + z_1(2) \\ Y_{23} =& z_1(1)\cos q_2 + \dot{q}_1 z_2(1)\sin q_2 \end{aligned}$$

where

$$z_1 = \begin{bmatrix} z_1(1) \\ z_1(2) \end{bmatrix} = J^{-1}(q)\left(\ddot{x} - \dot{J}J^{-1}\dot{x}\right)$$

$$z_2 = \begin{bmatrix} z_2(1) \\ z_2(2) \end{bmatrix} = J^{-1}(q)\dot{x}$$

and $J(q)$ denotes the Jacobian matrix of the robot. At the initial time, the link length and mass of each manipulator were estimated as $\hat{m}_1(0) = \hat{m}_2(0) = 0.8$ kg and $\hat{l}_1(0) = \hat{l}_2(0) = 0.2$ m. Then, the estimated parameter vector $\hat{\theta}(0)$ for each robot at the initial time could be determined by (50). The control gains were chosen to be

$$\begin{aligned} \Lambda =& \text{diag}\{10\}\ (1/\text{s}) \\ k_r =& \text{diag}\{1\}\ (\text{N}\cdot\text{m}\cdot\text{s/rad}) \\ \beta =& \text{diag}\{100\}\ (1/\text{s}) \\ k_\epsilon =& \text{diag}\{1\}\ (\text{N}\cdot\text{m/rad}\cdot\text{s}) \\ \Gamma =& \text{diag}\{0.1\}. \end{aligned}$$

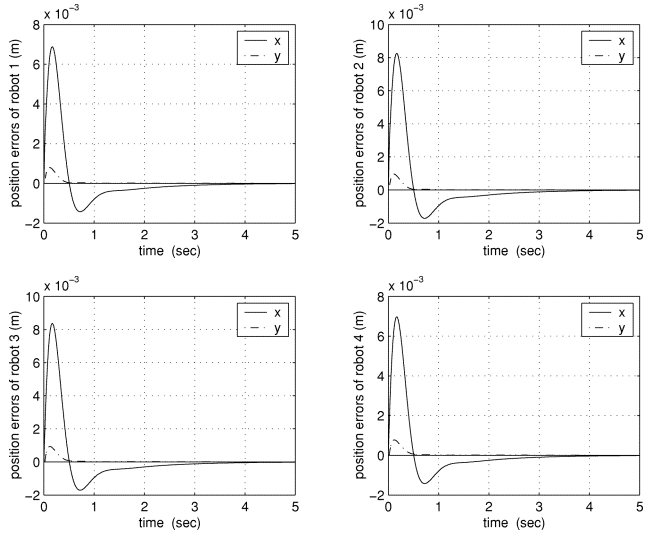

Fig. 9. Position errors of robots with adaptive synchronized control.

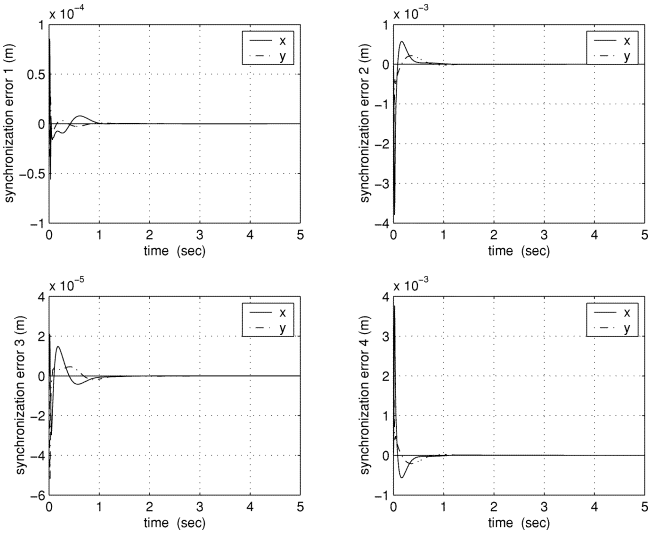

Fig. 10. Synchronization errors with adaptive synchronized control.

Fig. 9 illustrates position tracking errors of the robots with the proposed adaptive synchronized control, where solid lines and dashdot lines denote coordinates in x and y directions, respectively. In addition to satisfactory position-tracking convergence, there appears to be good performance in position synchronization amongst four robots, as shown in Fig. 10. Figs. 11 and 12 illustrate tracking responses with the independent adaptive control without synchronization (namely $\beta = 0$ and $k_\epsilon = 0$), for comparison. The major difference between results with the two methods lies in the synchronization error. It can be seen through comparison of Figs. 10 and 12 that the proposed synchronized

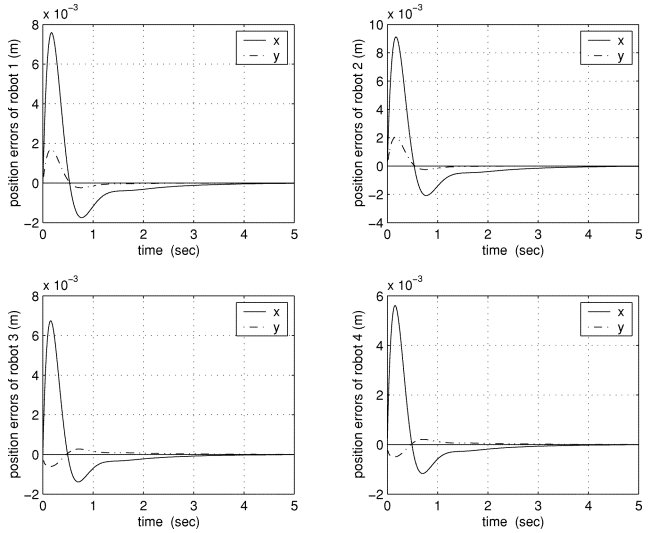

Fig. 11. Position errors of robots with independent adaptive control without synchronization.

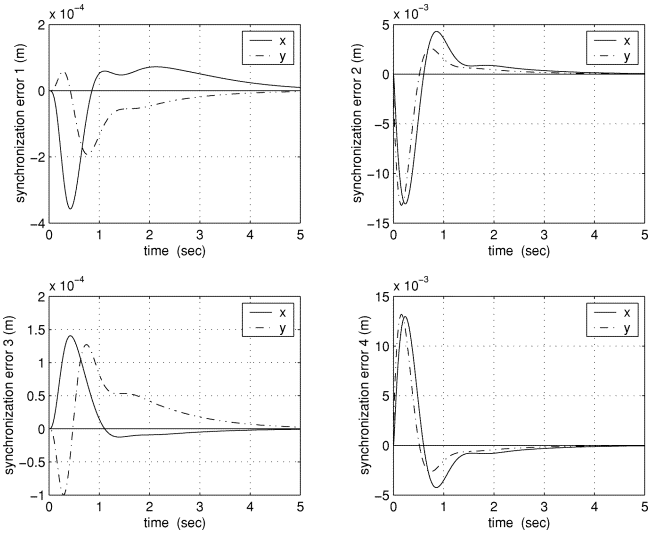

Fig. 12. Synchronization errors with independent adaptive control without synchronization.

controller can effectively reduce the transient position synchronization error, while causing the position-tracking error to converge to zero.

We then tested the system by adding a force disturbance $1N-m$ to robot 1 from 0.5–0.75 s during the motion. Figs. 13 and 14 illustrate position errors and synchronization errors of the robots, respectively, with the proposed synchronization control. These results are different from those in Figs. 9 and 10, due to adding the force disturbance in the motion. It is seen that although only robot 1 is subject to the force disturbance, the other three robots have corresponding responses in the position tracking to avoid large synchronization errors. (Large synchronization errors are not allowable in the coordination task.) Figs. 15 and 16 illustrate results with the independent adaptive control without synchronization. Except robot 1, position errors of robot $2\sim4$ in Fig. 15 are the same as those in Fig. 11, since there is no force disturbance acting on these robots. The large transient position error of robot 1 results in significant increment

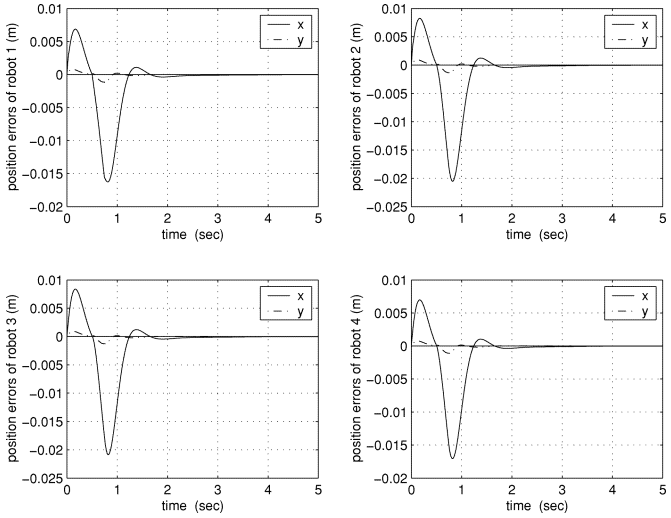

Fig. 13. Position errors of robots with adaptive synchronized control (with disturbance).

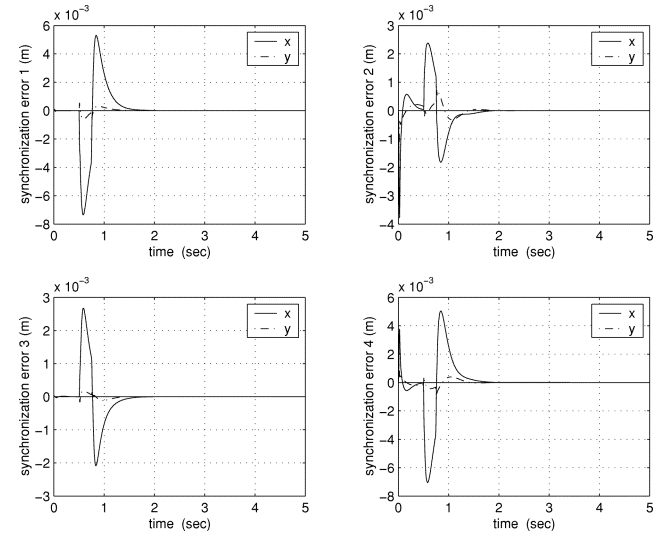

Fig. 14. Synchronization errors with adaptive synchronized control (with disturbance).

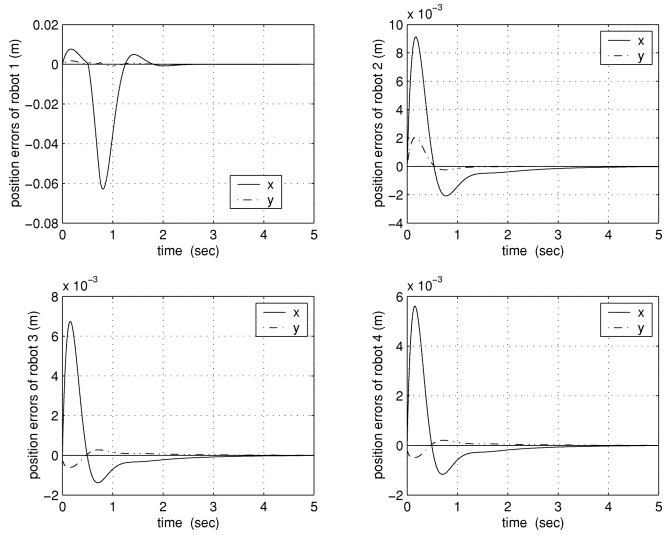

Fig. 15. Position errors of robots with independent adaptive control without synchronization (with disturbance).

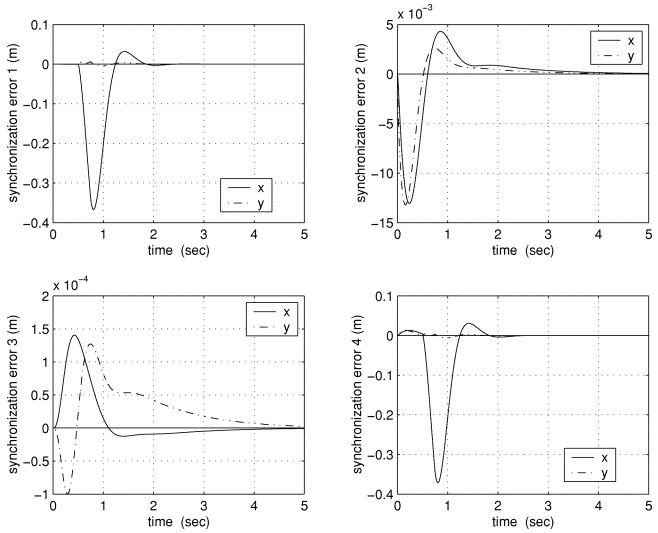

Fig. 16. Synchronization errors with independent adaptive control without synchronization (with disturbance).

of synchronization errors $\epsilon_1(t)$ and $\epsilon_4(t)$, as shown in Fig. 16. This may cause a serious problem in the coordination task. Note that the synchronization errors $\epsilon_2(t)$ and $\epsilon_3(t)$ in Fig. 15 are the same as those shown in Fig. 11, since $\epsilon_2(t)$ and $\epsilon_3(t)$ are not affected by $e_1(t)$ based on definitions in (48).

VI. Conclusions

A new adaptive synchronized control algorithm is proposed for coordination of multiple manipulators in assembly tasks. Each robot is required to track its desired trajectory while maintaining a certain kinematic relationship with the other robots, through motion synchronization. Failure to maintain this relationship in tracking may cause the system to be damaged or the assembly task to fail. The proposed coordination strategy is to stabilize position tracking of each manipulator while synchronizing motions of all manipulators by causing differential position errors of every pair of manipulators to converge to zero. In the control design, we incorporate the cross-coupling technology into an adaptive control structure. It has been shown that the proposed adaptive synchronized controller guarantees asymptotic convergence to zero of both position errors and synchronization errors. The proposed coordination scheme is of a decentralized architecture, and is more straightforward and easier to implement. Experiments on coordinating two CRS A460 industrial robots and simulations on a four-robot assembly work cell demonstrate the effectiveness of the proposed approach.

References

[1] S. Arimoto, F. Miyazaki, and S. Kawamura, "Cooperative motion control of multiple robot arms or fingers," in *Proc. IEEE Int. Conf. Robotics and Automation*, 1987, pp. 1407–1412.

[2] K. Kosuge *et al.*, "Decentralized coordinated motion control of multirobots," in *Proc. RSJ Annu. Conf.*, 1993, pp. 705–706.

[3] L. Feng, Y. Koren, and J. Borenstein, "Cross-coupling motion controller for mobile robots," *IEEE Trans. Contr. Syst. Technol.*, pp. 35–43, Dec. 1993.

[4] D. Gauthier, P. Freeman, G. Carayannis, and A. Malowany, "Interprocess communication for distributed robotics," *IEEE Trans. Robot. Automat.*, vol. RA-3, pp. 493–504, Dec. 1987.

[5] P. Hsu, "Control of multi-manipulator systems: Trajectory tracking, load distribution, internal force control and decentralized architecture," in *Proc. IEEE Int. Conf. Robotics and Automation*, 1989, pp. 1234–1239.

[6] T. Kamano, T. Suzuki, N. Iuchi, and M. Tomizuka, "Adaptive feedforward controller for synchronization of two axes positioning system," *Trans. Soc. Instrum. Contr. Eng.*, vol. 29, no. 7, pp. 785–791, 1993.

[7] A. J. Koivo and M. A. Unseren, "Reduced order model and decoupled control architecture for two manipulators holding a rigid object," *ASME J. Dynam. Syst., Meas. Control*, vol. 113, pp. 646–654, 1991.

[8] Y. Koren, "Cross-coupled biaxial computer controls for manufacturing systems," *ASME J. Dynam. Syst., Meas. Control*, vol. 102, pp. 265–272, 1980.

[9] Y. Koren and C. C. Lo, "Advanced controllers for feed drives," in *Proc. Annu. CIRP*, 1992, pp. 689–698.

[10] P. K. Kulkarni and K. Srinivasan, "Cross-coupled control of biaxial feed drive servomechanisms," *ASME J. Dynam. Syst., Meas. Control*, vol. 112, no. 2, 1990.

[11] H. C. Lee and G. J. Jeon, "A neuro-controller for synchronization of two motion axes," *Int. J. Intell. Syst.*, vol. 13, pp. 571–586, 1998.

[12] Y. H. Liu, S. Arimoto, and T. Ogasawara, "Decentralized cooperation control: Non-communication object handling," in *Proc. IEEE Int. Conf. Robotics and Automation*, 1996, pp. 2414–2419.

[13] P. R. Moore and C. M. Chen, "Fuzzy logic coupling and synchronized control of multiple independent servo-drives," *Control Eng. Practice*, vol. 3, no. 12, 1995.

[14] D. Sun and J. K. Mills, "Performance improvement of industrial robot trajectory tracking using adaptive-learning scheme," *ASME J. Dynam. Syst., Meas. Control*, vol. 121, no. 2, pp. 285–292, June 1999.

[15] T. J. Tarn, A. K. Bejczy, and X. Yun, "Coordinated control of two arms," in *Proc. IEEE Int. Conf. Robotics and Automation*, 1986, pp. 1193–1202.

[16] M. Tomizuha, J. S. Hu, and T. C. Chiu, "Synchronization of two motion control axes under adaptive feedforward control," *ASME J. Dynam. Syst., Meas. Control*, vol. 114, no. 6, pp. 196–203, 1992.

[17] J. T. Wen and K. K. Delgado, "Motion and force control of multiple robotic manipulators," *Automatica*, vol. 28, no. 4, pp. 729–743, 1992.

[18] N. Xi, T. J. Tarn, and A. K. Bejczy, "Intelligent planning and control for multirobot coordination: An event-based approach," *IEEE Trans. Robot. Automat.*, vol. 12, pp. 439–452, June 1996.

[19] L. F. Yang and W. H. Chang, "Synchronization of twin-gyro precession under cross-coupled adaptive feedforward control," *J. Guid. Control Dyn.*, vol. 19, no. 3, pp. 534–539, 1996.

[20] T. Yoshikawa, T. Sugie, and M. Tanaka, "Dynamic hybrid position/force control of robot manipulator-controller design and experiment," *IEEE Trans. Robot. Automat.*, vol. 4, pp. 699–705, Dec. 1988.

[21] X. Yun, N. Sarkar, and V. Kumar, "Dynamic control of 3-D rolling contacts in two-arm manipulation," *IEEE Trans. Robot. Automat.*, vol. 13, pp. 364–376, June 1997.

[22] Y. F. Zheng and J. Y. S. Luh, "Control of two coordinated robots in motion," in *Proc. IEEE Int. Conf. Robotics and Automation*, 1985, pp. 1761–1766.

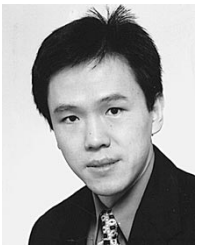

Dong Sun (S'95–M'00) received the B.Sc. and M.Sc. degrees in mechatronics from Tsinghua University of Beijing, Beijing, China, and the Ph.D. degree in robotics and automation from the Chinese University of Hong Kong, Shatin, in 1997.

He worked with the University of Toronto, Toronto, ON, Canada, as a post-doctoral researcher and Agile System Inc., Waterloo, ON, Canada, as an R&D engineer. In January 2000, he returned to Hong Kong to join the Department of Manufacturing Engineering and Engineering Management, City University of Hong Kong, Kowloon, as an Assistant Professor. His research interests lie in robotics and automation, mechatronics, and motion controls. He has served as reviewer or programme committee member for a number of international journals and conferences.

Dr. Sun received the National Education Commission of China's Science and Technology Progress Award in 1995, the Alexander von Humboldt Fellowship from Germany in 1996, an Industrial Research Fellowship of Natural Science and Engineering Research Council from Canada in 1999, and Innovation and Technology Fund from Hong Kong in 2001. He is a professional engineer in Ontario.

James K. Mills (S'81–M'82) received the Bachelor's degree from the University of Manitoba, Winnipeg, MB, Canada, and the Master's degree from the University of Toronto, Toronto, ON, Canada, in 1980 and 1982, respectively, both in electrical engineering. He received the Ph.D. degree from the University of Toronto in 1987 in robotic control.

He worked in industry in a consulting company and assisted in the development of a low-cost inertial attitude and heading reference unit for use in an underwater tow-body. He then worked at DSMA International Ltd., ON, Canada, and worked on the conceptualization of a number of projects related to aircraft wind-tunnel testing. He was appointed an Assistant Professor in the Department of Mechanical and Industrial Engineering, University of Toronto, in 1988 and rose through the ranks to Full Professor in 1997. His research interests include robot control, control of multirobots, control of flexible link robots, design of actuators, localization, development of fixtureless assembly technology, design and control of high-speed machines, development of neural network controllers, etc. He has published over 180 journal and conference papers, and supervised over 40 master's and Ph.D. students and a number of postdoctoral fellows and research engineers. He has been an Invited Visiting Professor at the Centre for Artificial Intelligence and Robotics in Bangalore, India. He has completed a three-year term as Associate Chair of the Department of Mechanical and Industrial Engineering, University of Toronto, and made significant advances in the development of a new mechatronics curriculum and funding for that program.